Eng. & Tech. Journal, Vol. 29, No. 5, 2011

High Resolution Miniaturized Lens Arrays Scanners and Image Formation Systems For Medical Applications

Samira M. Arif*, Dr. Mohamed S. Ahmed**
&Dr. Dayah N. Raouf**

Received on: 2/11/2010
Accepted on: 3/2 /2011

Abstract

The optical design of miniaturized high resolution micro lens arrays systems MLAs, for scanning and image formation, is achieved. The types of scanner systems that have been handled are microlens array MLA scanner system with f-number $F_{\#}$ 2.54, for two scanning angles. The one with higher scanning angle predicts the influence of increasing aberrations on the output. The imaging capabilities of single and multiple array systems are presented. Their performance characteristics are studied and analyzed to fit medical applications, the most important are compactness and resolution. The overall size of the designed systems is a fraction of a centimeter and the resolution is in a few micrometers regime. However, it is found that optimizations are needed to enhance the quality of images, specifically for larger scanning angles.

Keywords: micro optics, optical scanner, optical design

تصميم منظومات مسح وتصوير عاليه التفريق ذات مصفوفات من العدسات المصغره المايكرويه للتطبيقات الطبيه

الخلاصة

تم أنجاز تصاميم بصريه لمنظومات مسح وتصوير مصغره عاليه التفريق ذات مصفوفات من العدسات المايكرويه. تتكون منظومه المسح المعالجه من مصفوفه عدسات مايكرويه ذات عدد بؤرى يساوى 2.54 وذلك لقيمتين من زوايا المسح. أظهرت زاويه المسح الاعلى تأثيرا اكبر للزيوغ على خرج المنظومه. وتم عرض القدره التصويريه لكل من المنظومه مفرده المصفوفه والمتعدده المصفوفات، وكذلك دراسه وتحليل مواصفات الاداء للمنظومات متعدده المصفوفات لتلائم التطبيقات الطبيه، اهمها الحجم وقدره التفريق. الحجم الكلى للمنظومه المصممه هو جزء من السنتيميتر وقدره التفريق بعض مايكروميترات. ومع ذلك فقد وجد ان المنظومات فى حاجه الى التحسين للحصول على صور ذات جوده افضل خاصه عند زوايا المسح الاعلى.

الكلمات الدالة : البصريات المايكرويه, الماسحات البصريه, التصاميم البصريه

Introduction

Miniaturized optical systems are of importance for many various applications; of special concern are the medical applications. Laser camera system, capsular endoscopes, and confocal microscopes are few examples, where tiny optical scanners and imaging systems play an important role [1-3].

Microlens arrays are implemented in optical systems for steering and for Image formation, the archetype of its design is the compound eye of insects[4,5].

In this work the optical designs of miniaturized single array of microlenses MLA system for imaging, and multiple microlenses arrays MLAs systems for scanning and imaging, are presented. In section two the basic design principles of MLAs for

* Ministry of Sciences and Technology / Baghdad
** Applied Sciences Department, University of Technology / Baghdad

https://doi.org/10.30684/ etj.29.5.5
University of Technology-Iraq, Baghdad, Iraq/2412-0758

scanning and imaging, are explained. For the optical configurations studied, system components dimensi-ons, system geometry and optical constraints are chosen based on geometrical and physical optical considerations to fulfill the performance objectives. However, zemax software[6] is exploited for geometrical ray tracing, physical optical propagation, and non-sequential ray tracing. Section three is devoted for the results and analysis of these optically designed systems. The influence of various design parameters on the quality of scanned beams and images, are studied.

Conclusions extracted out of the Results are presented in section four.

Single microlens array MLA imager system

The capability of a single MLA for multiple imaging is demonstrated in Fig.1, using the non-sequential ray tracing facilities of zemax[6], for 5x5 lens array system. Degradation of quality of generated images (specifically contrast of images) outwardly is clear.

Multiple microlens arrays MLAs scanner and imaging systems

A decentered lens arrays in afocal Keplerian telescopic system, are used for scanning light beams[1]. It is demonstrated in Fig.2 implementing three stacks of microlens arrays MLAs systems. MLA_2 and MLA_3 are decentered with respect to MLA_1 that cause the deflection of light beam.

Alternatively, another design was used to simplify the mechanical cons-truction and alignment of the optical scanner, imaging system[7]. This model is designed and shown in Fig.3, where the second microlens array MLA_2 is joined with the third array MLA_3 by sharing the same substrate of refractive index n to construct a doubly sided microlens arrays DMLA. A collimated beam of light is to be incident on the first microlens array MLA_1. The final focusing lens is to focus the collimated beam out of MLA_3 toward the last image plane. The designed data parameters of this system is given in table-1.

Design and Analysis

The design of two models of micro optical array scanners and imaging systems, with f-numbers $F_{\#}$ 6.8 and $F_{\#}$ 2.54 are demonstrated in Fig.4 and Fig.5, respectively. For these two models the design data parameters are given in table-2 and table-3.

The focal length, of lenses of the system with $F_{\#}$ 2.54 is relatively large so the scanning angles are small, that produces a narrow field of view. This design is to be studied for two values of scanning angles, or alternatively decenteration values(r_o) of the doubly microlens array DMLA. These values are r_o=0.05mm and r_o=0.065mm, which correspond to scanning angles of 1.6^o and 2.079^o, respectively.

In Fig.6(A) the point Spread Functions PSFs are shown at the image plane for the case of r_o=0.0, which shows a maximum value of Strehl ratio of value S=1. While at the scanning position with decenteration r_o=0.05mm, Strehl ratio reduced to S=0.969. The same type of analysis curves are shown in Fig.6 (B) for the case of decenteration r_o=0.065mm. The Strehl ratio of this scanning position reduced to a low value of S=0.657. Also, one notices that the peak intensity of PSF is reduced, other orders appear with significant intensity. This leads to a reduction in contrast, but keeps the width of PSFthesame thus resolution are not affected. The case with larger

decenteration is worser, considering the Modulation Transfer Functions MTFs curves as is shown in Fig.7, where spot diagrams and MTF curves are shown for both decenteration values. The maximum diffraction limited resolution is $590mm^{-1}$ corresponding to a minimum resolution of 1.6μm.

The physical optics propagation algorithm is applied on this system, to trace and demonstrate the light field distribution at the intermediate (Mid) focusing plane of the first microlens array, and at the image plane, as shown in Fig.8 (a) and (b), respectively. As it is clear from these diagrams, the focusing is not optimum, it is close but not totally exact. Also, by applying this program it is possible to trace the irradiance distribution for the three scanning positions r_o=0.0,±0.065mm at the image plane, as is shown in Fig.9.

To analyze the capability of these microlens arrays scanner systems MLAs for imaging, the same scanner model with $F_{\#}$ 2.54 is applied with decenteration amount r_o of values 0.05mm and 0.065mm. In Fig.10(A), (B), and (C), the results of decenteration with r_o=0.05mm, are presented. The intermediate images of the letter F are shown at the mid focusing plane in Fig.10(A)a, of the first microlens array. The number of images corresponds to the number of lenslets(5x5) that first microlens array consists of with a lens width=0.15mm(in both directions x and y). Final image for the letter F is formed at the image plane in(A)b, using an imaging or focusing lens. The images shown at the image plane is inverted for a Keplerian telescopic type scanner system. The scanning positions at mid plane (B)c and at image plane (B)d are shown in Fig.10(B) for all decenteration values of r_o= 0.0,±0.05mm, while the MTF curve for both cases on axis r_o=0.0 and off axis r_o=±0.05mm are presented in Fig.10(C)e, and f, respectively.

To compare these results with the case of decenteration value r_o=±0.065mm, Fig.11 illustrates the same set of characteristics curves shown in Fig.10, but now the decenteration is 0.065mm instead of 0.05mm. The results indicate that images are degraded due to two reasons. First, that as the scanning angle get larger, actually it is the maximum close to the radius of lenslet which is 0.075mm, the edges of images are cut out in the two off axis scan positions(±0.065mm decentertion values). Second, the MTF curves are far from the diffraction limit performance.

The images of letter F at image plane at three scan positions are shown in Fig.11B for decenteration values of 0.065mm. There are a noticeable differences between the two scan positions for the two scan values 0.05 mm and 0.065mm, shown in Fig.10 and Fig.11, respectively.

To make the effects of these differences even more clear on images, the letter F used in the previous analysis is replaced by a group of Alphabet letters from A to Z. Fig.12(a) illustrates the image quality of Alphabet group at image plane for on axis decenteration r_o=0.0mm, while Fig.12(b) shows the images for the three scanned positions at the image plane in off axis positions, where decenteration values are r_o=0.0,±0.05mm. In comparison with the image appeared in Fig.12(c) that corresponds to the same analysis of

images but now the decenteration values are r_o=0.0,±0.065mm, the images quality and shapes reflect the following facts: the two scanned images with decenterations r_o=±0.065mm are more distant to each other in comparison to that of the two scanned positions corresponding to decenterations r_o=±0.05mm. Also, two lines of the Alphabet set disappeared from these off axis image positions, as they get closer to the edges of the lenslet, and for the increasing effects of aberrations toward the outward edge of lenses.

Conclusions

The imaging capabilities of an optical micro scanner system with $F_{\#}$ 2.54 are demonstrated based on the model of afocal Keplerian telescopic system. Also, this system is analyzed at various scanning angles, or decenteration values of the doubly microlens array DMLA. It is concluded that at higher decenteration values the system is not performing at the diffraction limit, as MTF curves and images predict. PSF curves indicate reduction in its value(low contrast) at higher scanning angles. Therefore, optimization steps are to be taken to improve the quality of these images. One might notice as well, that in all final images, formed at the image plane and studied so far, there are always a traces of some parts of other surrounding images. This occurs because many design parameters, one is image plane position, are not optimized to make all the multiple intermediate images appear at a single exact position.

However, the micro optical system designed is still of high resolution that fit for many medical applications such as in compact laser camera system (implemented with surgery tube), and endoscopes.

References

[1] A. Akatay, C. Ataman, and H. Urey, ‘‘High resolution beam steering using microlens arrays’’, Optics Letters, vol. 31, no. 19, 2006.

[2] R. Moshe, ‘‘encapsulated medical imaging device and method ’’, United States Patent Application 20030208107, Publication Date 11/ 06/2003.

[3] S. Kwon, and L.P. Lee, ‘‘Micromachined transmissive scanning confocal microscope ’’ , Optics Letters, vol. 29, no. 7, 2004.

[4] H. Yahya, ‘‘ The fly’s eye is a source of inspiration for new medical imaging system’’, http://www.harunyahya.com/m_science_news.php. 2009

[5] J. Duparrè, P. Dannberg, P. Schreiber, A. Bräuer, and A. Tünnermann, ‘‘Artificial apposition compound eye fabricated by micro optics technology’’, Applied Optics, vol. 43, no. 22, pp.4303-4310, 2004.

[6] Software for optical design; zemax Development Corporation, 2005.

[7] A. Akatay, and H. Urey,‘‘ Design and optimization of microlens array based high resolution beam steering system’’, Optics Express, vol.15, no.8, 2007.

Table (1) Data parameters of complete Afocal Keplerian telescopic MLA scanner system.

$F_{\#}$ = 0.92 (image space)	Radius of curvatures for MLA1 R_1= -- , R_2= + mm DMLA R_3 = 1mm, R_4 = -1mm
Entrance Pupil Diameter ENPD=2.5mm	Wavelength λ = 0.532μm
Material glass BK7 , n= 1.51	f_1= 1.925mm, f_2=2.3 mm
Conic=0.0 for all surfaces	Thickness of MLA1=0.04mm , DMLA=2.92mm
NA=0.476(image space)	Total track = 8.685mm (object- image planes)
Arrays lens numbers , 3x3	Width of lenslets in x, y directions , 0.7x0.7mm

Table (2) Data parameters of designed MLA scanner system with $F_{\#}$ 6.8.

$F_{\#}$ = 6.8 (image space)	Radius of curvatures R_1= R_2 = R_3 = 0.0929mm
ENPD=0.39mm	Wavelength λ = 0.532μm
Material glass BK7 , n= 1.51	f_1=f_2= 0.148mm
Conic=0.0 for all surfaces	Thickness of 1st MLA=0.03mm,2nd MLA=0.27mm
NA=0.07(image space)	Total track= 1.048mm
Arrays lens numbers , 9x9	Width of lenslet in x, y directions , 0.1x0.1mm

Table (3) Data parameters of designed MLA scanner system with $F_{\#}$ 2.54

$F_{\#}$ = 2.54 (image space)	Radius of curvatures R_1=0.9298mm R_2 = R_3 = 0.923mm
ENPD=0.71mm	Wavelength λ = 0.532μm
Material glass BK7 , n= 1.51	$f_1=f_2$= 1.79mm
Conic k_1= -2.308 , k_2 = k_3 = 0.0	Thickness of1st MLA=0.15mm,2nd MLA=2.7mm
NA=0.19 (image space)	Total track= 8.4mm
Arrays lens numbers , 5x5	Width of lenslet in x, y directions 0.15x0.15mm

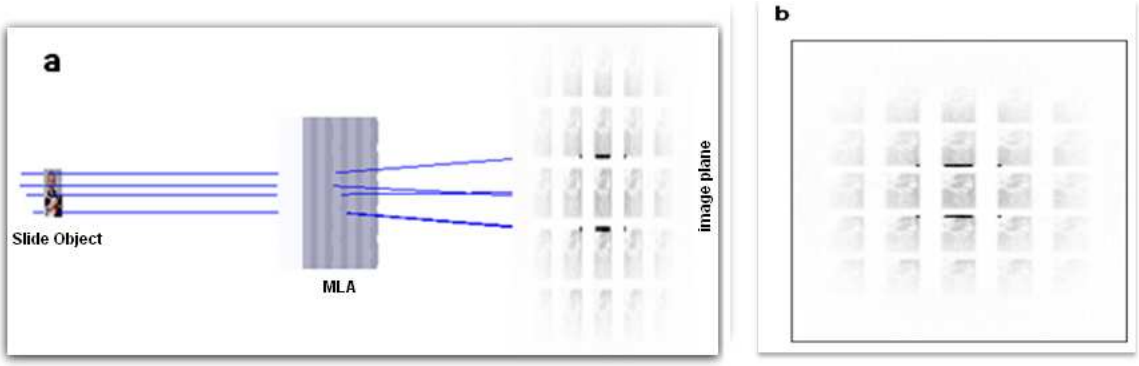

Detector Image: Incoherent Irradiance

Figure (1) Image formation of a slide object using non- sequential ray tracing (a) layout of array of microlens MLA imaging system, (b) images as appeared at image plane.

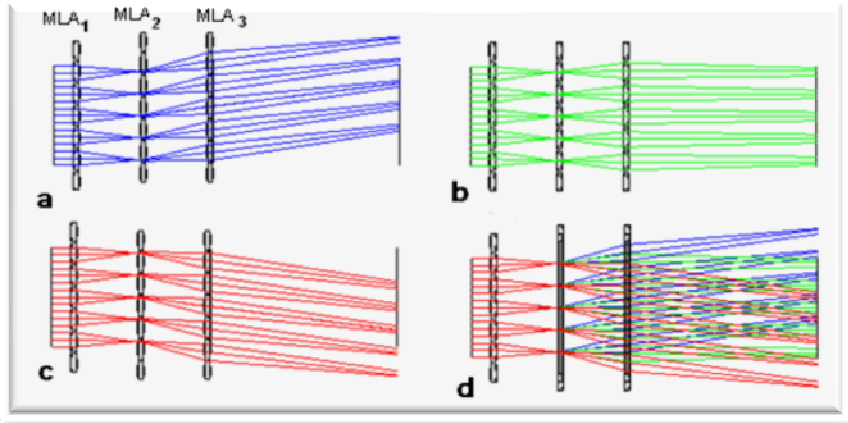

Figure (2) Three separated MLAs scanner system, a) MLA_2 and MLA_3 are decentered upward with respect to the optical axis of MLA_1. b) With no decenteration. c) Downward decenteration. d) all simultaneous cases (a, b, and c).

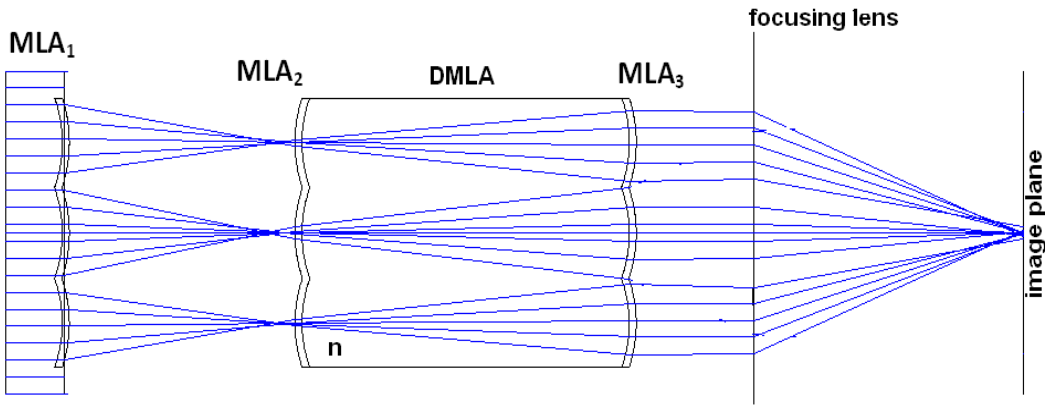

Figure (3) Layout of complete Afocal Keplerian telescopic system (Implementing three sequential MLAs).

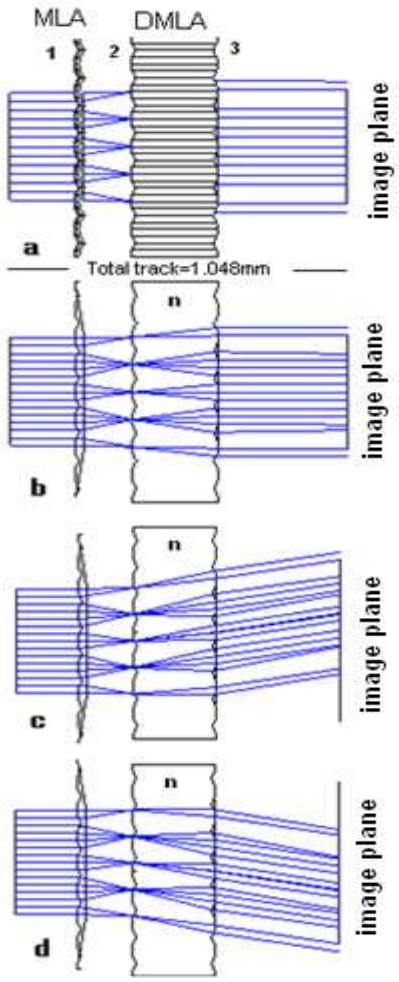

Figure (4) layout of MLA scanner system with $F_{\#}$ 6.8. a) r_o =0.0(solid), b) r_o =0.0, c) r_o = +0.03mm, d) r_o = - 0.03mm.

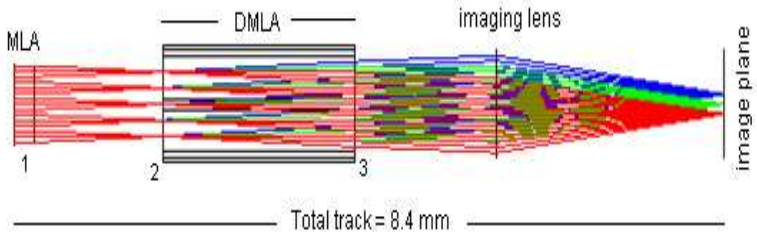

Figure (5) Layout of MLA scanner system with $F_{\#}$ = 2.54, for all three scanning angles, simultaneously.

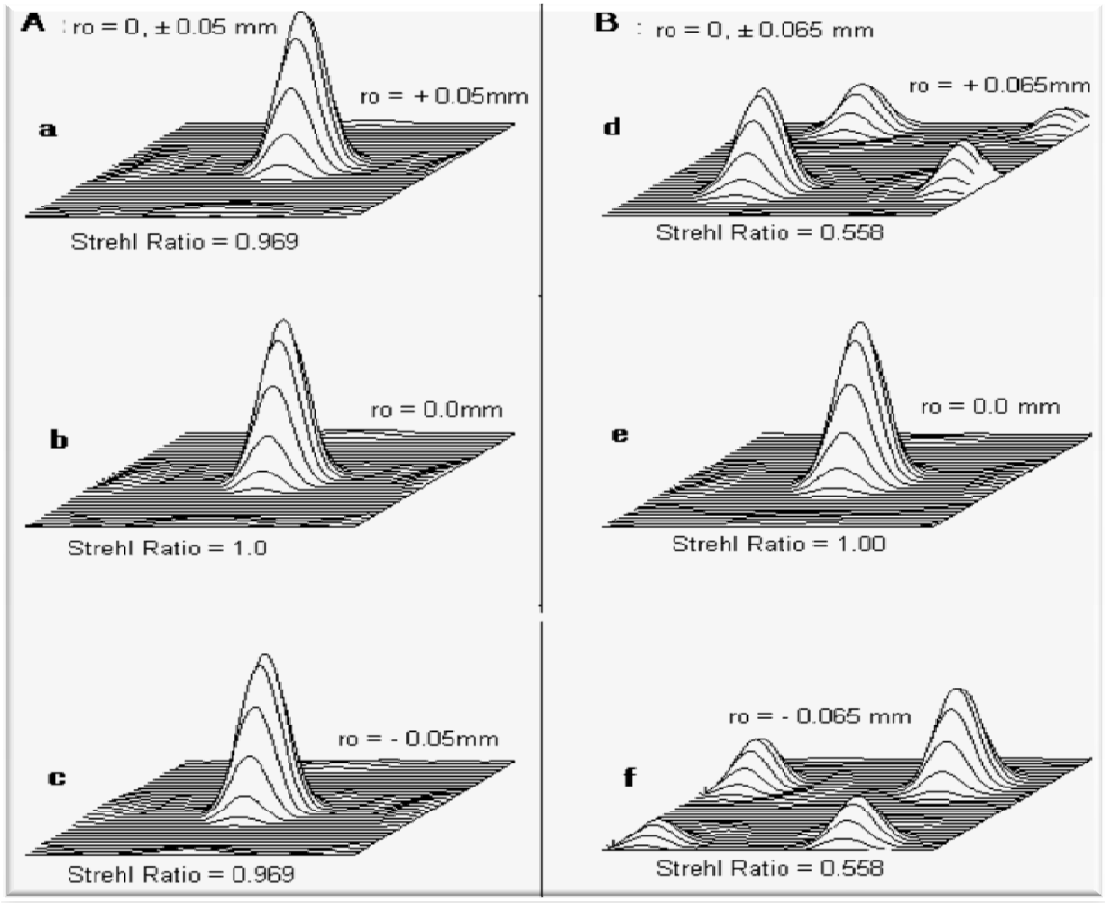

Figure (6) Point Spread Functions PSFs, of MLAs scanner system $F_{\#}$ 2.54, with decenteration in (A) for r_o = 0, ±0.05mm, a) +0.05mm, b) 0.0mm, c) – 0.05mm, B) for r_o = 0, ±0.065mm, d) +0.065mm, e) 0.0mm, f) - 0.065mm.

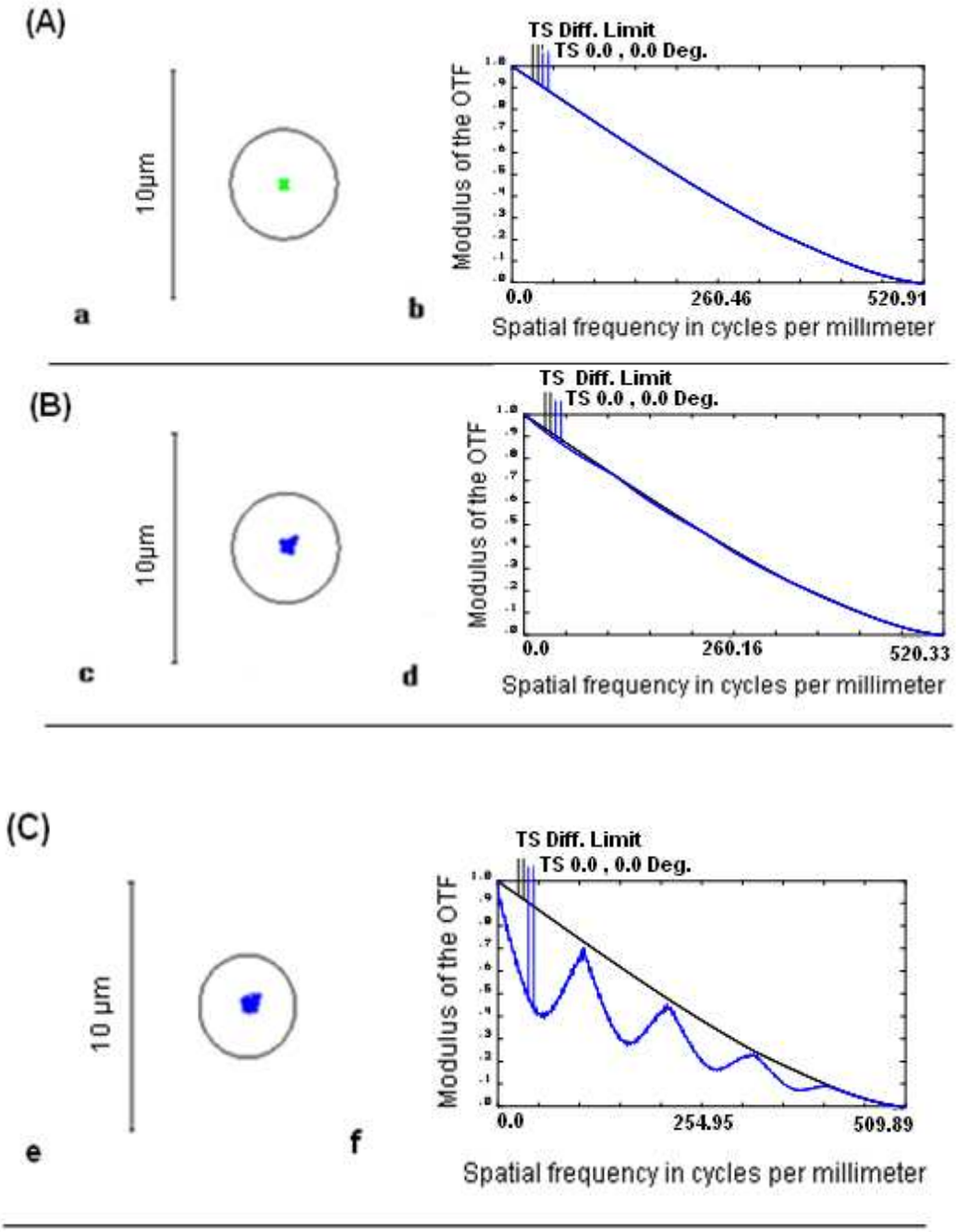

Figure (7) Spot diagrams and MTF curves of MLAs scanner system, $F_{\#}$ 2.54, (A) r_o= 0.0mm, (B) r_o= 0.05mm, (C) r_o = 0.065mm. (the circle around the spot diagrams refer to the Airy disc)

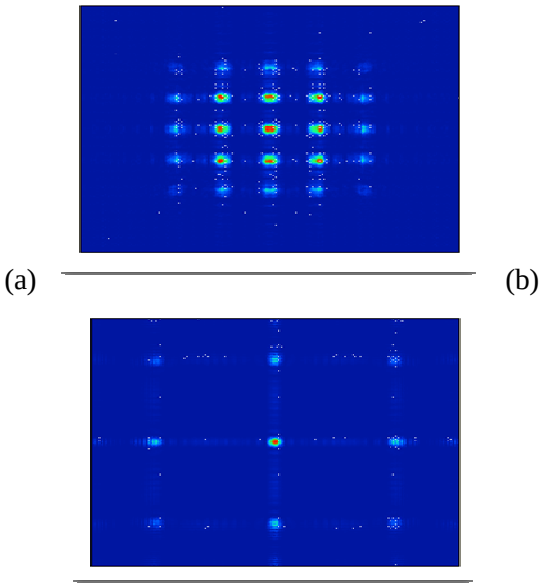

Figure 8 (a) Irradiance field distribution at (Mid) focusing plane of first MLA (5x5), of MLAs scanner($F_{\#}$ 2.54) , (b) Irradiance field distribution at the image plane.

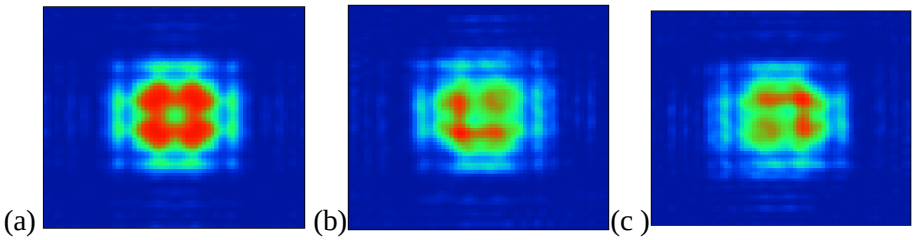

Figure 9 $F_{\#}$ 2.54 MLAs scanner with DMLA decenteration r_o = 0.0 , ±0.065mm, where
a)r_o= 0.0mm, b) r_o = +0.065mm , and c) r_o = - 0.065mm.

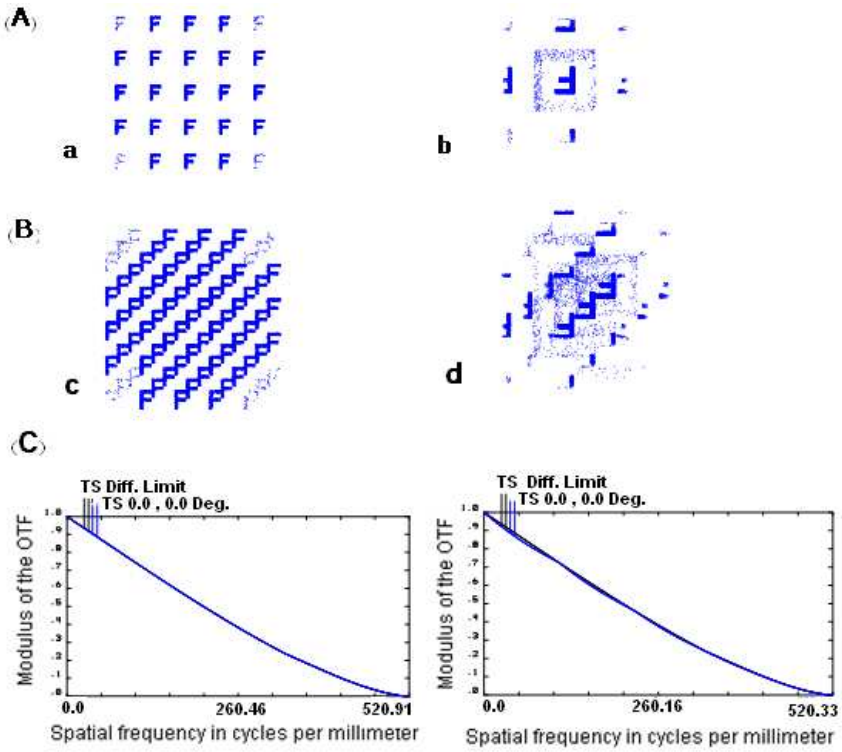

Figure (10) MLA scanner system, (A) image formation at r_o = 0.0, a) mid fousing plane, b) image plane, (B) image formation at r_o = 0.0, ± 0.05mm , c) mid focusing plane, d) image plane, (C) MTF for e) r_o = 0.0, f) r_o = 0.05mm.

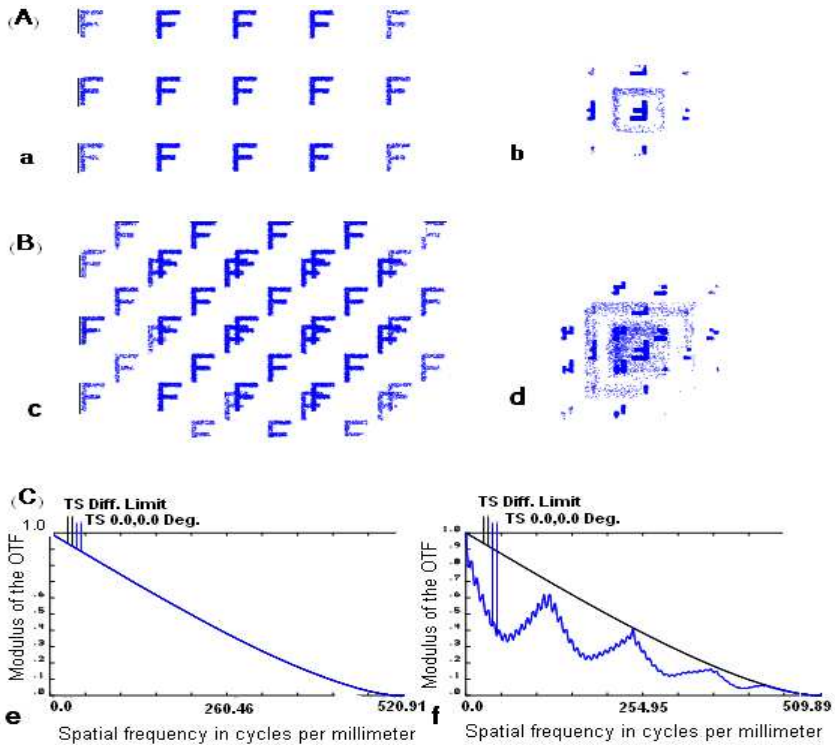

-

Figure (11) MLA scanner system, (A) image formation at r_o = 0.0, a) mid fousing plane, b) image plane, (B) image formation at r_o =± 0.065mm , c) mid focusing plane, d) image plane, (C) MTF for e) r_o = 0.0, f) r_o = 0.065mm.

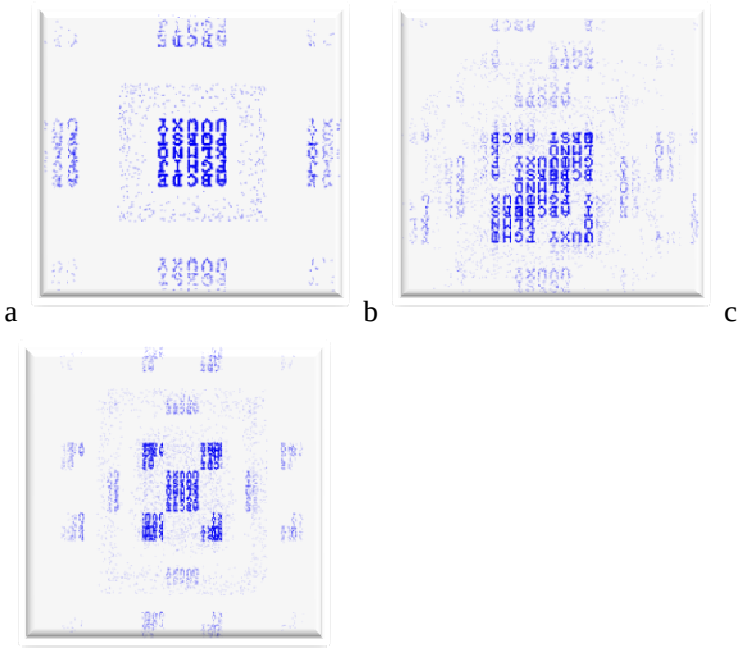

Figure (12) Image formation of Alphapet letters by MLA system $F_{\#}$ 2.54, with (a) r_o=0.0mm, (b) r_o=0.05mm, (c) r_o=0.065mm.